Temperature-dependent magnetic anisotropy in the layered magnetic semiconductors CrI_3 and $CrBr_3$

Nils Richter,[1,2] Daniel Weber,[3] Franziska Martin,[1] Nirpendra Singh,[4] Udo Schwingenschlögl,[4,*] Bettina V. Lotsch,[3,†] and Mathias Kläui[1,2,‡]

[1]*Johannes Gutenberg-Universität, Institut für Physik, Staudinger Weg 7, 55128 Mainz, Germany*
[2]*Graduate School Materials Science in Mainz, Staudingerweg 9, 55128 Mainz, Germany*
[3]*Max-Planck-Institut für Festkörperforschung, Heisenbergstraße 1, 70569 Stuttgart, Germany*
[4]*Physical Sciences and Engineering Division (PSE), King Abdullah University of Science and Technology (KAUST), Thuwal 23955-6900, Saudi Arabia*

(Received 14 April 2017; published 20 February 2018)

Chromium trihalides are layered and exfoliable semiconductors and exhibit unusual magnetic properties with a surprising temperature dependence of the magnetization. By analyzing the evolution of the magnetocrystalline anisotropy with temperature in chromium iodide CrI_3, we find it strongly changes from $K_u = 300 \pm 50\ \mathrm{kJ/m^3}$ at 5 K to $K_u = 43 \pm 7\ \mathrm{kJ/m^3}$ at 60 K, close to the Curie temperature. We draw a direct comparison to $CrBr_3$, which serves as a reference, and where we find results consistent with literature. In particular, we show that the anisotropy change in the iodide compound is more than 3 times larger than in the bromide. We analyze this temperature dependence using a classical model, showing that the anisotropy constant scales with the magnetization at any given temperature below the Curie temperature, indicating that the temperature dependence can be explained by a dominant uniaxial anisotropy where this scaling results from local spin clusters having thermally induced magnetization directions that deviate from the overall magnetization.

DOI: 10.1103/PhysRevMaterials.2.024004

I. INTRODUCTION

The materials class of layered chromium (Cr) trihalides CrX_3, with X being a halogen ion of fluorine (F), chlorine (Cl), bromine (Br), or iodine (I), has experienced revived attention recently with numerous publications on their magnetic properties [1–7]. Due to their layered structure with weak van der Waals bonds between the layers, they belong to those materials where exfoliation is possible, and the prospect of magnetic monolayer systems is a source of the renewed interest. Only recently, Huang *et al.* demonstrated that ferromagnetism persists down to a monolayer of chromium iodide, which marks a milestone in the research of two-dimensional magnetic materials [5]. In all CrX_3 compounds, the magnetic properties are closely tied to the details of the crystalline structure. Bulk CrX_3 crystals all exhibit a phase transition from monoclinic ($AlCl_3$ type, space group $C2/m$) at elevated temperatures to trigonal (BiI_3 type, space group $R\bar{3}$) at cryogenic temperatures [3,6,7]. For both cases, the layers extend in the ab plane and are stacked along the c axis. Hansen [8], Tsubokawa [9], and Dillon, Jr. [10,11] have pioneered the work on magnetism in these compounds, finding them to be one of the rare instances where superexchange leads to ferromagnetism instead of antiferromagnetism. With their unusual magnetic properties and the possibility of existing in monolayer form, chromium trihalides are promising materials for ultrathin spintronics [12]. While there are a number of publications dealing with optical properties and resonance studies of these materials [13–15], much work has focused on the chemical synthesis. Now that the fabrication of high-quality CrX_3 crystals has been established, a careful analysis of the magnetic properties can be attempted in order to address the remaining open questions [3,6], where one of these questions is the stabilization of ferroic order in layered two-dimensional systems such as CrX_3 [5]. The magnetocrystalline anisotropy is for the moment the most promising ingredient that can allow one to overcome the limitations set by the Mermin-Wagner theorem [16], which prohibits magnetic ordering in two or less dimensions. Here, we focus in particular on the magnetic anisotropy of CrI_3 and $CrBr_3$. Since the magnetic properties of bulk samples serve as a basis for the understanding of magnetic phenomena in reduced dimensions, e.g., in few- or monolayer samples of CrX_3, a profound understanding of these compounds is evidently needed, especially considering that magnetic monolayers of CrI_3 have now become accessible [5]. The bromide compound has been studied in some detail, with Tsubokawa (to our knowledge) having been the first to quantify the uniaxial anisotropy constant by torque magnetometry [9], and Dillon, Jr. has provided the temperature dependence using ferromagnetic resonance (FMR) [10,17]. In comparison, CrI_3 has not been studied thoroughly. For instance, to the best of our knowledge, Ref. [11] is the only experimental determination of the magnetocrystalline anisotropy constant in CrI_3. Moreover, even though the compound exhibits a surprising temperature dependence of the magnetization (see discussion below), so far only the saturation field has been discussed without probing the value of the anisotropy constant, which is the key property that

*udo.schwingenschlogl@kaust.edu.sa
†b.lotsch@fkf.mpg.de
‡klaeui@uni-mainz.de

governs the anisotropic magnetic behavior [3,8]. In order to facilitate the understanding of magnetism in CrX_3 compounds, we demonstrate in this paper how the temperature dependence of the anisotropy in CrI_3 can be ascertained, showing a strong decrease as a function of increasing temperature. We directly compare the results for CrI_3 to those measured in $CrBr_3$, where we confirm the value and temperature dependence given in the literature and show that the same is much stronger in the iodide. To understand this temperature dependence of the anisotropy, we demonstrate that for both CrI_3 and $CrBr_3$, it is consistent with a scaling law. The critical exponent found then allows us to use a classical model to explain the magnetization as a function of temperature as resulting from a dominant uniaxial anisotropy, with local spin-cluster directions deviating from the overall magnetization direction due to thermal activation.

II. METHODS

A. Sample preparation

$CrBr_3$ and CrI_3 were prepared directly from the elements in an evacuated quartz tube similar to reports from literature [9]. Great care was taken to ensure the spatial separation of the reactants within the ampoule prior to heating. The halogen was kept slightly above room temperature, allowing the vapors to react with the metal at the hot zone at 1023 K. In the presence of a small excess of halogen, crystals grew at the cool end of the ampoule in the natural temperature gradient due to a chemical transport reaction.

B. Magnetometry

After preparing and loading a CrI_3 crystal or a $CrBr_3$ crystal into a superconducting quantum interference device (SQUID) magnetometer (QuantumDesign MPMS XL), we measure the projection of the magnetic moment along the (vertical) z direction at variable temperatures. Additionally weighing the crystals using a laboratory balance (Kern ABT 220–5DM) allows for the calculation of mass and resulting magnetization M, which is the measured magnetic moment divided by the volume. The small size of the crystals implies a low mass (typical mass is in the low-milligram regime), resulting in the largest contribution to the absolute measurement error of the magnetization. However, relative changes exhibit comparatively low errors, allowing us to deduce robust conclusions, for instance, about the temperature dependence. Furthermore, we do not consider effects of demagnetization because the impact of possible effective magnetic surface charges is negligible due to the bulk nature of our samples and therefore shape anisotropy plays no role.

C. Ab initio calculations

Density functional theory is employed by means of the full-potential linearized augmented plane-wave method of the WIEN2K code [18]. The generalized gradient approximation of Perdew, Burke, and Ernzerhof is used for the exchange-correlation potential. Brillouin zone integrations are performed on a $8 \times 8 \times 8$ mesh. The atomic sphere sizes of Cr and I are set to 2.5 Bohr radii and the plane-wave cutoff parameters to $R_{\mathrm{Kmax}} = 8$ and $G_{\mathrm{max}} = 12$. We use the experimental lattice

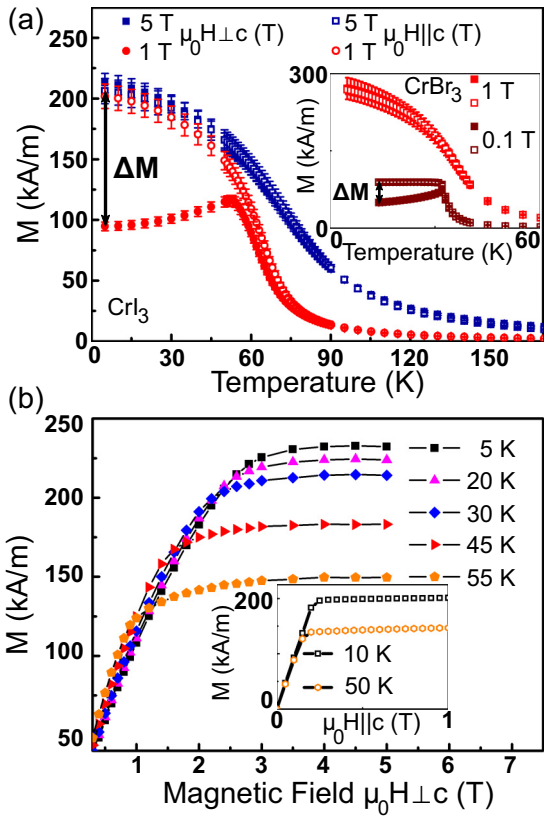

FIG. 1. (a) Temperature dependence of the magnetization in CrI_3. (solid markers: $H \perp c$; open markers: $H||c$). For small fields ($\leqslant 1$ T), the magnetocrystalline anisotropy leads to a strong difference of the effective saturation value for the different configurations and, below 50 K, to a decrease of M with decreasing temperature for $H \perp c$ (see main text). The inset shows the same measurement for $CrBr_3$. (b) Positive branch of magnetic hysteresis loops for CrI_3 between 5 K and 55 K in the $H \perp c$ configuration. The saturation field H_{sat} is extracted from these curves and used to calculate the magnetocrystalline anisotropy. The inset shows for comparison the $H||c$ configuration at 10 K (black) and 50 K (pink). Error bars are omitted for the sake of clarity.

constants ($a = 6.867$ Å, $c = 19.807$ Å) from Ref. [3] and relax the atomic coordinates until the atomic forces have declined below 0.001 eV/Å. This procedure allows us to obtain the key structural information, namely, the crystal structure that governs all electronic and magnetic properties.

III. RESULTS

In Fig. 1(a) we present the magnetization M of CrI_3 as a function of temperature for two different measurement configurations ($H||c$ and $H \perp c$) and at different field magnitudes of $\mu_0 H = 1$ T and 5 T. Below the Curie temperature T_C (between 61 K [3,6] and 68 K [11] for CrI_3) we observe with further decreasing temperature an increase of M which saturates eventually at liquid helium temperatures. When we apply a field of 5 T, M saturates at a value of $M_{S,5T} = 206.1 \pm 10.3$ kA/m, irrespective of whether $H||c$ or $H \perp c$. This saturation magnetization corresponds to a magnetic moment of $3.00 \pm 0.15\ \mu_B$/F.U., where μ_B denotes

the Bohr magneton and F.U. stands for formula unit, in perfect agreement with the expected saturation moment in CrI_3 [3,11]. However, for a smaller field of 1 T, M saturates at the same value only in the $H||c$ configuration, while in the $H \perp c$ configuration, M remains at a significantly smaller saturation value of $M_{S,1T}^{\text{perp}} = M_{S,1T}^{\text{parallel}} - \Delta M = 94.7 \pm 3.5\,\text{kA/m}$. Generally, such a difference ΔM can be attributed to the effect of the magnetocrystalline anisotropy and here, the c axis is found to be the easy axis. If one looks at the temperature dependence of the magnetization in the plane, a surprising decrease of the magnetization below 50 K is observed, which cannot be explained by constant magnetocrystalline anisotropy and requires a more complex analysis as detailed below. In $CrBr_3$, the c axis is also the easy axis, while the magnitude of the anisotropy is clearly lower [see inset of Fig. 1(a)]. As shown in the inset, for the bromide 1 T is enough to saturate M in both configurations at $M_{S,1T} = 271 \pm 21\,\text{kA/m}$ (equivalent to $3.09 \pm 0.24\ \mu_B$/F.U.). Here, a discrepancy between M_S in the different configurations as explained above already for CrI_3 occurs only at lower fields, for example, at 100 mT. Although 100 mT is also not sufficient to fully saturate the sample even in the configuration $H||c$, the behavior is qualitatively similar to the iodide compound. While $M(T)$ monotonously increases with decreasing temperature for $H||c$, a decrease of M with decreasing temperature is found below 30 K for 0.1 T applied in the plane perpendicular to the c axis.

In order to explain the unusual magnetization behavior discussed above which cannot be reproduced with the conventional assumption of a temperature-independent anisotropy, we ascertain the impact of the magnetocrystalline anisotropy now in detail by analyzing magnetic hysteresis loops [Fig. 1(b)] at different temperatures. In the inset of Fig. 1(b), we observe for $H||c$ a sharp rise of the magnetic moment with increasing field, followed abruptly by a state of saturation when a certain magnetic field H_{sat} is reached. Increasing the temperature (while staying below T_C) does not change this behavior, except that the saturation occurs at a lower magnetization. In Fig. 1(b), we show only the positive branches of the hysteresis loops, as within the measurement accuracy (800 A/m), it is neither possible to observe a remanent magnetization nor a coercive field H_C, thus setting an upper limit of $H_C \leqslant 800$ A/m.

For CrI_3 the hysteresis loops start to open slightly at 5 K; however, remanence and coercivity are still small at this temperature. Hence, CrI_3 and $CrBr_3$ are magnetic extraordinarily soft materials, where the magnetization follows the applied magnetic field direction virtually instantaneously during reversal, and obviously not even pinning centers for domain walls in the crystal structure lead to a remanent net magnetization at zero field. This observation is consistent with previous reports [3], and we suggest that one possible reason lies in the small interlayer exchange coupling of 1.8 K in CrI_3 and 0.5 K in $CrBr_3$ [19]. For CrI_3 this energy scale is 2.7 times lower than the lowest measurement temperature used here, leading to a vanishing interlayer coupling and thus to an immediate randomization of the magnetization between all layers, even though the magnetic coupling within individual layers is strong. In order to observe a remanent net magnetic moment and the resulting coercive field for the stacked system, the low-field regime should be revisited, ideally using remanence-free Helmholtz coils instead of superconducting ones and measured at millikelvin temperatures, which is, however, beyond the scope of this work and not possible with our current setup. Nevertheless, future investigations including thickness-dependent measurements could shed light on this currently not completely understood issue.

We repeat the hysteresis loops in the $H \perp c$ configuration, which show distinct differences as compared to the parallel configuration. First, the slope of $M(H)$ in the low-field regime, i.e., the magnetic susceptibility $\chi = dM/dH$, is smaller. Furthermore, the curves measured at different temperatures clearly intersect, which is a consequence of a reduction in H_{sat} with increasing temperature. The magnetic field H_{sat} is a direct measure of the magnetocrystalline anisotropy, which contributes to the total micromagnetic energy density with a term $E_A = K_u \sin^2(\theta - \varphi)$. In this formula, K_u denotes the uniaxial anisotropy constant, θ the direction of the preferred magnetization, and φ the direction in which the magnetization points, and when $\theta - \varphi = 90^\circ$ (which is the case for $H \perp c$) the effect of the magnetocrystalline anisotropy becomes maximal. If we consider the sample being fully magnetized above H_{sat}, the single-domain state becomes a valid approximation, which can be described by the Stoner-Wohlfarth model [20]. Within this model, the anisotropy constant can be derived via

$$\frac{2K_u}{M_S} = \mu_0 H_{\text{sat}}, \tag{1}$$

with μ_0 denoting the vacuum permeability. This relation allows us to deduce K_u as a function of temperature below T_C for both CrI_3 and $CrBr_3$ (Fig. 2). However, one needs to obtain the saturation magnetization M_S and the saturation field H_{sat} in order to calculate K_u from Eq. (2). Experimentally, we extract both quantities from the magnetization curves taken in the $H \perp c$ configuration as follows: First, we consider a straight line parallel to the magnetic field axis fitted to the magnetization data above a magnetic field of 3 T, where the system is well above the saturation threshold. Second, we determine dM/dH in the low-field regime of the same curve. The intersection point of these two lines yields the saturation field as its abscissa and the saturation magnetization as its ordinate. In Fig. 2(c), we plot our measurement of the temperature dependence of $CrBr_3$'s anisotropy together with the temperature dependence extracted from Ref. [10]. For the whole temperature range we find an excellent agreement, corroborating the validity of Eq. (1), where the low-T anisotropy amounts to $K_u = 86 \pm 6\,\text{kJ/m}^3$. For CrI_3, this is the first determination of a T dependence in K_u. As in $CrBr_3$, the anisotropy decreases towards T_C. At 5 K, the experimental value is $K_u = 301 \pm 50\,\text{kJ/m}^3$.

For CrI_3, where no published in-depth reports are available as a reference, we compare the experimental value of the anisotropy with numerical calculations based on density functional theory, which have been executed by the full-potential linearized augmented plane-wave method of the WIEN2K code [18]. To understand the origin of the magnetic properties, we calculate, as one of the key features of the system, the crystallographic structure. Based on the experimentally determined lattice constants ($a = 6.867$ Å, $c = 19.807$ Å) [3], we first model the crystal structure and check the stability. The relaxed atomic coordinates reproduce the experimental values with very good accuracy, as shown in Table I.

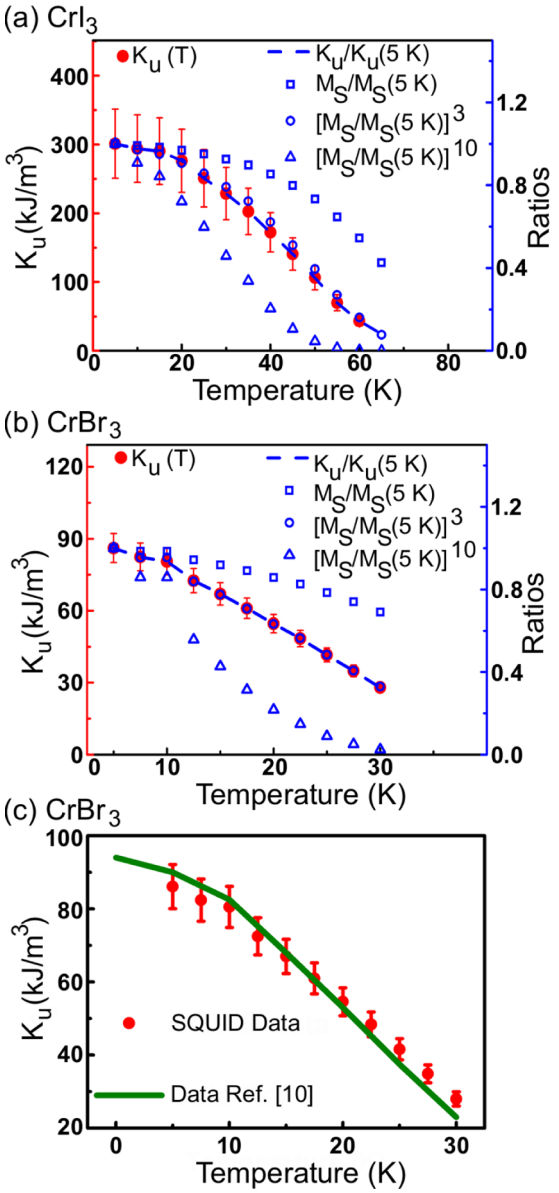

FIG. 2. (a), (b) Temperature dependence of K_u for CrI_3 and $CrBr_3$. Left axes: For CrI_3 as well as for $CrBr_3$ a decrease of K_u is clearly visible as T is increased towards T_C. Right axes: The ratio $K_u(T)/K_u(5\,\mathrm{K})$ plotted in comparison to the ratio $[M_S(T)/M_S(5\,\mathrm{K})]^{n(n+1)/2}$, where $n = 1$, 2, and 4. For both compounds, the anisotropy scales to the third power of $M_S(T)/M_S(5\,\mathrm{K})$, in line with theoretical expectations for a predominant uniaxial anisotropy (leading to $n = 2$). Error bars of the ratios are omitted for the sake of clarity. In (c), we show the temperature dependence of K_u for $CrBr_3$ in comparison with the temperature dependence for the anisotropy extracted from Ref. [10], where we find excellent agreement.

As the next step, we evaluate the total energies for magnetization along the a and c axes. The resulting energy difference of 0.5 meV divided by the unit-cell volume yields the theoretically expected anisotropy constant. We find that the experimental value coincides with this calculated expectation of $K_u^{\mathrm{theo}} = 290\ \mathrm{kJ/m^3}$, showing the validity of this approach. To analyze the temperature dependence of our anisotropy data, we consider that the magnetic anisotropy is a product of the interplay between the spontaneous magnetization and the crystal lattice. Often, the temperature dependence of the anisotropy is found to be stronger than that of the spontaneous magnetization. In a simple classical theory, anisotropy and magnetization are linked via the relation

$$\langle K^{(n)} \rangle \propto M_S^{\frac{n(n+1)}{2}}, \tag{2}$$

where $\langle K^{(n)} \rangle$ is the anisotropy expectation value for the n^{th} power angular function [21,22], in the case of uniaxial anisotropy $n = 2$ and of cubic anisotropy $n = 4$, leading to an exponent of 3 and 10, respectively. To check whether this model can describe our temperature dependence, we also show in Figs. 2(a) and 2(b) the experimentally determined temperature dependences plotted as $K_u/K_u(5\,\mathrm{K})$, $M_S/M_S(5\,\mathrm{K})$, $[M_S/M_S(5\,\mathrm{K})]^3$, and $[M_S/M_S(5\,\mathrm{K})]^{10}$. The comparison clearly shows that the scaling $\frac{K_u(T)}{K_{u,0}} = (\frac{M_S(T)}{M_{S,0}})^3$ is the most appropriate fit. This is in line with the predominant uniaxial anisotropy found by our magnetometry measurements and thus explains the temperature dependence of the uniaxial anisotropy in both systems, CrI_3 and $CrBr_3$. In the theory developed by Zener and Carr [21,22], the observed decrease of K_u with increasing temperature arises from solely from a large number of local spin clusters, fluctuating randomly around the macroscopic magnetization vector, activated by a nonzero thermal energy, while the anisotropy constants themselves are explicitly independent of temperature. These insights into the nature of the magnetocrystalline anisotropy are key for the understanding of ferromagnetism in CrX_3 compounds with a small number of layers. While in pure two-dimensional systems no magnetic order is expected [16], mechanical corrugations and magnetic anisotropy are possible pathways to establish magnetism in quasi-two-dimensional single CrX_3 layers nevertheless. While ferromagnetism has been shown to exist in a monolayer of CrI_3 [5], the magnetic properties of few- and monolayers of $CrBr_3$ and $CrCl_3$ are yet elusive. Like CrI_3, both of these other two compounds can be subjected to mechanical exfoliation. For $CrCl_3$, the exfoliation down to a double layer has been shown recently [7], and for $CrBr_3$ we conducted a set of cleavage experiments. For the procedure of mechanical exfoliation, we place the as-produced crystal on a piece of adhesive tape and exfoliate it at least 5 times (depending on the thickness of the initial crystal). In the last step, the tape with the crystals is pressed onto a heated substrate (120 °C) for 30 s. The resulting flakes with varying thicknesses on the substrate surface can be located using an optical microscope. Flakes with low optical contrast are expected to be thin and we further investigate these flakes using atomic force microscopy [Fig. 3(a)]. We readily find stable thin crystals, where the one shown in Fig. 3 has a thickness of approximately 6.7 nm corresponding to roughly ten layers [Fig. 3(b)]. With these

TABLE I. Experimental and theoretical atomic coordinates of Cr and I in CrI_3.

	Experiment [3]	Theory
Cr	1/3, 2/3, 0.33299	1/3, 2/3, 0.33286
I	0.31667, 0.33453, 0.41230	0.32313, 0.33467, 0.41327

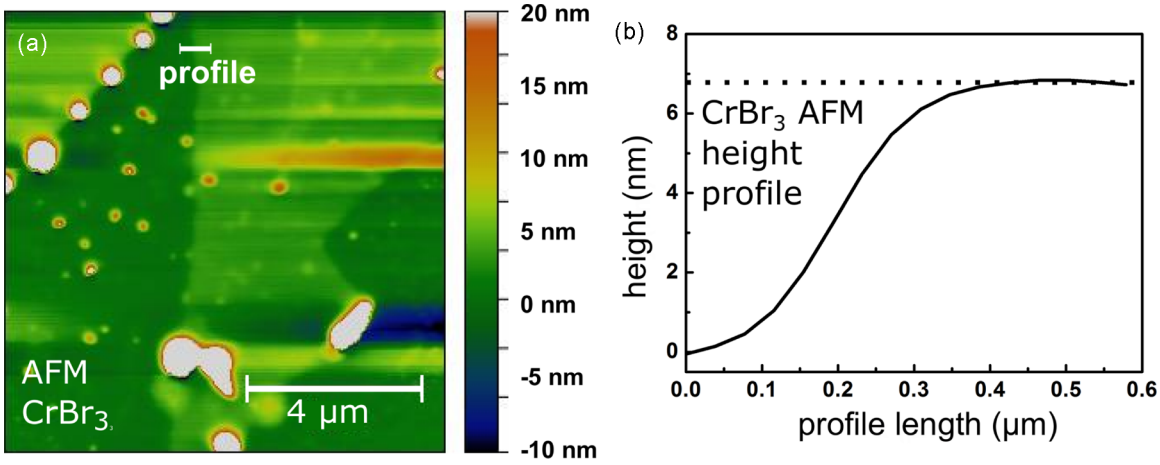

FIG. 3. Atomic force microscopy image of a $CrBr_3$ flake on a GaAs substrate (a). The line profile (b) reveals a thickness of approximately 6.7 nm, which corresponds to roughly ten layers.

experiments, we demonstrate that also for the bromide the way towards exploration of magnetism in the two-dimensional limit is accessible and it is now equipped with a solid understanding of the magnetocrystalline anisotropy.

IV. CONCLUSION

In summary, we carried out an in-depth analysis of the magnetocrystalline anisotropy in CrI_3 and in $CrBr_3$, revealing that the complex magnetization dependence on temperature results from temperature dependence of the magnetocrystalline anisotropy. While for $CrBr_3$ our data's agreement with previous experiments is excellent, we find a more than three times stronger temperature evolution of K_u in CrI_3. The experimentally obtained value at low temperature, $K_u = 301 \pm 50\,\mathrm{kJ/m^3}$, is within the error identical to a theoretically derived value, $K_u^{\mathrm{theo}} = 290\ \mathrm{kJ/m^3}$, for 0 K and agrees with a value determined by FMR. We find that the temperature dependence can be explained based on a classical model, leading to a scaling of the temperature dependence with a critical exponent that results from a dominant uniaxial anisotropy combined with thermal activation effects that locally lead to magnetization deviating from the ensemble value.

Even with this understanding of the bulk compounds, our results show that the phenomenology of magnetism in CrX_3 compounds still requires further exploration. For example, despite the strong ferromagnetic coupling within layers of CrX_3, global magnetic remanence is regularly absent. We explain this absence with the low interlayer coupling, calling for magnetometry in tailored setups, e.g., capable of reaching mK temperatures. To understand the bulk magnetic properties of chromium trihalide compounds is furthermore a key first step to using these compounds as single layers in spintronic applications, in particular as the anisotropy has a major influence for the stabilization of magnetic ordering in reduced dimensions.

ACKNOWLEDGMENTS

We thank Prof. Dr. Gerhard Jakob, Prof. Dr. Hartmut Zabel, and Prof. Dr. Hans-Joachim Elmers for stimulating and helpful discussions. The research reported in this publication was supported by funding from King Abdullah University of Science and Technology (KAUST). The work was further funded by the DFG (SFB TRR 173 Spin+X), and N.R. gratefully acknowledges the MAINZ Graduate School of Excellence (DFG GSC/266) as well as the Carl Zeiss Stiftung. D.W. and B.V.L. are grateful for support from the Max Planck Society, the University of Munich (LMU), the Cluster of Excellence Nanosystems Initiative Munich (NIM), and the Center of Nanoscience (CeNS).

[1] J. Liu, Q. Sun, Y. Kawazoe, and P. Jena, Phys. Chem. Chem. Phys. **18**, 8777 (2016).
[2] W.-B. Zhang, Q. Qu, P. Zhu, and C.-H. Lam, J. Mater. Chem. C **3**, 12457 (2015).
[3] M. A. McGuire, H. Dixit, V. R. Cooper, and B. C. Sales, Chem. Mater. **27**, 612 (2015).
[4] C. N. Avram, A. S. Gruia, M. G. Brik, and A. M. Barb, Phys. B (Amsterdam, Neth.) **478**, 31 (2015).
[5] B. Huang, G. Clark, E. Navarro-Moratalla, D. R. Klein, R. Cheng, K. L. Seyler, D. Zhong, E. Schmidgall, M. A. McGuire, D. H. Cobden, W. Yao, D. Xiao, P. Jarillo-Herrero, and X. Xu, Nature (London) **546**, 270 (2017).
[6] H. Wang, V. Eyert, and U. Schwingenschlögl, J. Phys.: Condens. Matter **23**, 116003 (2011).
[7] M. A. McGuire, G. Clark, S. KC, W. M. Chance, G. E. Jellison, Jr., V. R. Cooper, X. Xu, and B. C. Sales, Phys. Rev. Mater. **1**, 014001 (2017).
[8] W. N. Hansen, J. Appl. Phys. **30**, S304 (1959).
[9] I. Tsubokawa, J. Phys. Soc. Jpn. **15**, 1664 (1960).
[10] J. F. Dillon, Jr., J. Appl. Phys. **33**, 1191 (1962).
[11] J. F. Dillon, Jr. and C. E. Olson, J. Appl. Phys. **36**, 1259 (1965).
[12] C. Felser, G. H. Fecher, and B. Balke, Angew. Chem. Int. Ed. **46**, 668 (2007).

[13] J. F. Dillon, Jr., H. Kamimura, and J. P. Remeika, J. Phys. Chem. Solids **27**, 1531 (1966).
[14] R. W. Bené, Phys. Rev. **178**, 497 (1969).
[15] S. D. Senturia and G. B. Benedek, Phys. Rev. Lett. **17**, 475 (1966).
[16] N. D. Mermin and H. Wagner, Phys. Rev. Lett. **17**, 1133 (1966).
[17] J. F. Dillon, Jr., J. Phys. Soc. Jpn. **19**, 1662 (1964).
[18] P. Blaha, K. Schwarz, G. Madsen, D. Kvasnicka, and J. Luitz, WIEN2k: An Augmented Plane Wave Plus Local Orbitals Program for Calculating Crystal Properties, Technische Universität Wien, Austria (2001).
[19] L. J. De Jongh and A. R. Miedema, Adv. Phys. **50**, 947 (2001).
[20] E. C. Stoner and E. P. Wohlfarth, Philos. Trans. R. Soc. Lond. Ser. Math. Phys. Sci. **240**, 599 (1948).
[21] C. Zener, Phys. Rev. **96**, 1335 (1954).
[22] W. J. Carr, J. Appl. Phys. **29**, 436 (1958).